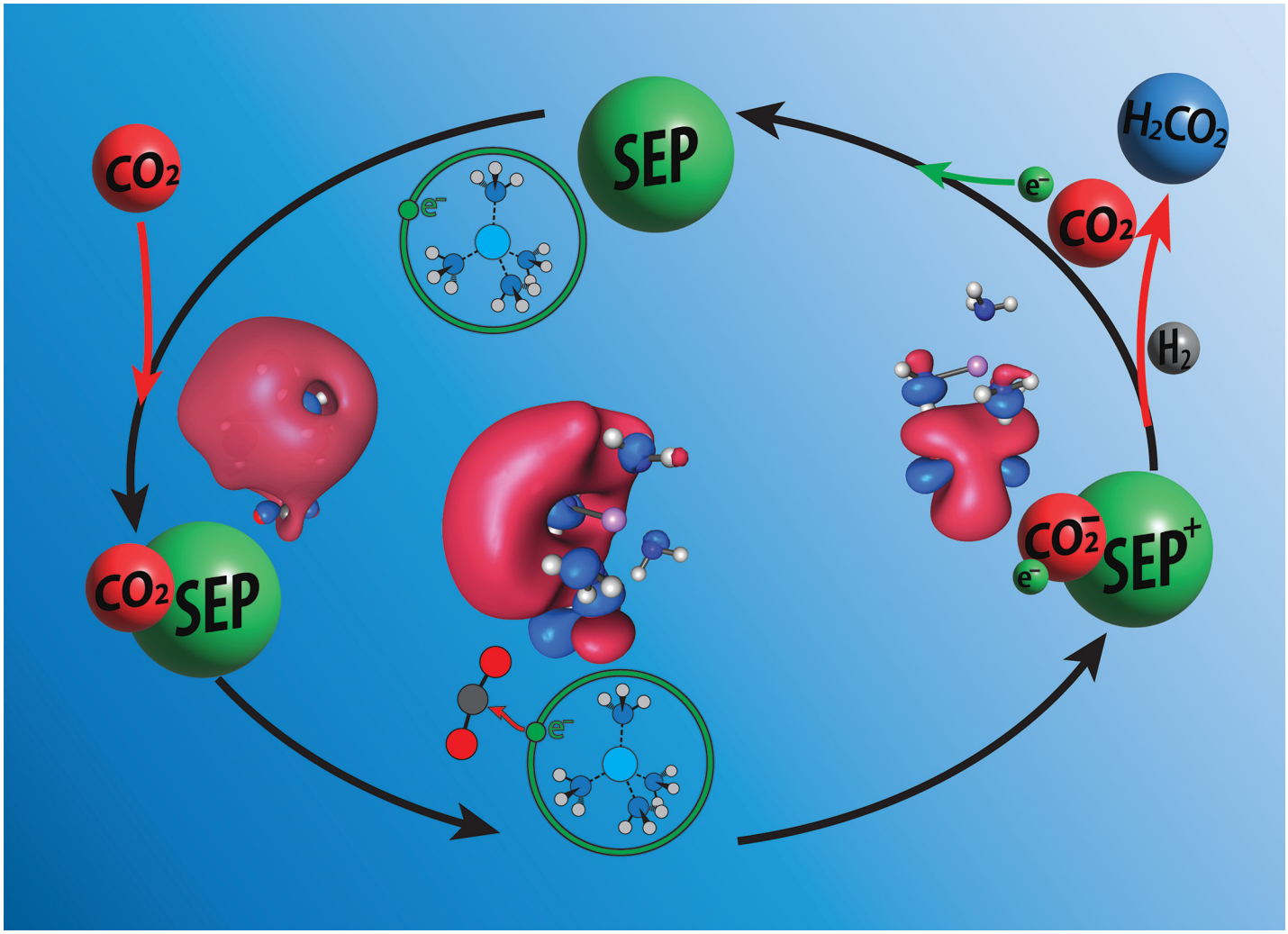

Showcasing research from Professor Evangelos Miliordos's laboratory, Department of Chemistry and Biochemistry, Auburn University, Auburn Al., USA.

Simultaneous CO_2 capture and functionalization: solvated electron precursors as novel catalysts

The application of solvated electron precursors (SEPs), metal complexes with diffuse electrons, in catalysis is studied mechanistically for the first time. These results demonstrate SEPs to be effective catalysts, capable of both capturing and functionalizing CO_2.

As featured in:

See Benjamin A. Jackson and Evangelos Miliordos, *Chem. Commun.*, 2022, **58**, 1310.

ROYAL SOCIETY OF CHEMISTRY

rsc.li/chemcomm

Registered charity number: 207890

ChemComm

ROYAL SOCIETY OF CHEMISTRY

COMMUNICATION

View Article Online
View Journal | View Issue

Cite this: *Chem. Commun.*, 2022, **58**, 1310

Received 26th August 2021,
Accepted 22nd December 2021

DOI: 10.1039/d1cc04748e

rsc.li/chemcomm

Simultaneous CO_2 capture and functionalization: solvated electron precursors as novel catalysts†

Benjamin A. Jackson and Evangelos Miliordos *

Metal complexes with diffuse solvated electrons (solvated electron precursors) are proposed as alternative catalysts for the simultaneous CO_2 capture and utilization. Quantum chemical calculations were used to study the reaction of CO_2 with H_2 and C_2H_4 to produce formic acid, methyldiol and δ-lactone. Mechanisms of a complete reaction pathway are found and activation barriers are reasonably low. The metal ligand complex readily reduces CO_2 and significantly stabilizes $CO_2^{\bullet-}$. Ligand identity minimally influences the reaction. Additional reactions and future strategies are proposed with the goal of inducing experimental interest.

Solvated electron precursors (SEPs) are a class of metal–ligand complexes consisting of a metal $M^{n+}(L)_x$ core surrounded by n metal electrons which are displaced to the periphery of the complex – these constitute the microscopic structure of solvated electron solutions in the dilute regime.[1] The study of SEPs poses an exciting avenue for the development of novel reduction catalysts. The diffuse nature of the outer solvated electron orbital is highly reactive while functionalization of SEP ligands suggests a potentially high degree of tunability and a wide range of applications.

Solvated electrons are powerful reducing agents capable of reducing benzene rings as evidenced in the well-known Birch reduction.[2] Previous experimental work in SEP reactivity has illustrated the ability of metal SEP hydrates to reduce O_2, CO_2, CH_3CN, and NO.[3–6] However, the mechanism of this reduction remains poorly understood. To this end, two gas-phase reaction systems involving the SEP $Li(NH_3)_4$ are mechanistically studied: the conversion of CO_2 and H_2 to formic acid/methyldiol and that of CO_2 and ethene to δ-lactone. In addition, SEP ligand effects are explored using ammonia, methylamine, ethylamine, water, and methanol.

The capture and utilization of CO_2 has been the topic of intense interest in the literature. A review of the used methods/materials is beyond the scope of this communication, but it is worth mentioning that practical applications involve two different molecular systems, one for the capture and one for the catalytic transformation of CO_2 to a platform chemical. For example, the work of Prakash and co-workers employed a polyamine system to capture CO_2 and a Ru-based catalyst for its conversion to methanol.[7–9] The present work reveals that SEPs can perform both tasks simultaneously.

The transition states (TS), reactants, intermediates, and products for the two gas-phase reaction systems were generally optimized in Gaussian 16[10] under density functional theory (DFT) using the CAM-B3LYP functional and the cc-pVTZ (Li, N, O, C) and aug-cc-pVTZ (H) basis sets.[11–14] This functional and basis set combination has been shown to provide accurate structures in SEP systems.[15,16] Augmentation of C and O basis sets is shown to minimally effect reaction energetics (see Fig. S10, ESI†). All optimal structures were of doublet spin multiplicity. Select structures were optimized at second-order Moller–Plesset perturbation theory (MP2) level and double-ζ basis sets.[17] Coupled-cluster singles, doubles, and perturbatively connected triples, CCSD(T), calculations were also obtained using Molpro 2015.5.[18,19] See the ESI† for a detailed discussion of computational methodology. The higher level CCSD(T) results were used to benchmark CAM-B3LYP energies for $Li(NH_3)_4$ and $Li(H_2O)_4$ which on average agree within ±1.5 kcal mol^{-1} (see Fig. S2 and S3 of ESI†).

The $Li(NH_3)_4$ complex consists of a $Li(NH_3)_4^+$ core which is surrounded by a pseudospherical diffuse orbital occupied by a single electron. The reaction pathway of $Li(NH_3)_4$ and CO_2 + $2H_2$ is given in Fig. 1. Electronic energies are used for all figures in this manuscript and free energy diagrams at 1 atm and 298 K are given in the ESI† and discussed below. The pathway begins with the coordination of CO_2 to the SEP with a binding energy of 1.7 kcal mol^{-1} (CO_2r). Following this is a transition state (eTS1) involving the transfer of the SEP electron to CO_2 to form the radical $CO_2^{\bullet-}$(CO_2p). The electronic energy activation

Department of Chemistry and Biochemistry, Auburn University, Auburn, AL 36849-5312, USA. E-mail: emiliord@auburn.edu

† Electronic supplementary information (ESI) available: The Electronic Supplementary Information file contains a more detailed description of the computational methodology. In addition, it provides optimal CAM-B3LYP geometries, harmonic vibrational frequencies, energetics for all intermediates and transition states, and free energy and enthalpy plots for the H_2 and C_2H_4 pathways. See DOI: 10.1039/d1cc04748e

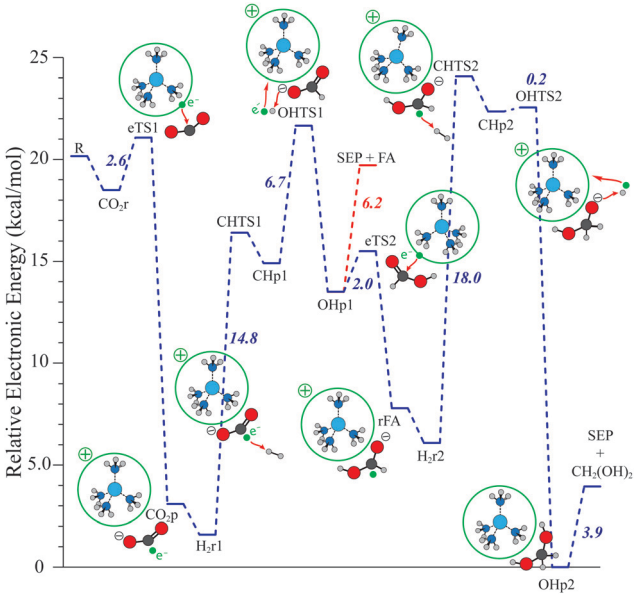

Fig. 1 Reaction pathway of $Li(NH_3)_4$ + CO_2 + 2 H_2 → $Li(NH_3)_4$ + $CH_2(OH)_2$. Graphical representations of transition states and select intermediates are given as figure insets. A green dot is used to indicate the movement of the SEP e^- throughout the pathway. Activation barriers are given in kcal mol^{-1}. Relative electronic energies are zeroed to the lowest point of the pathway. See Table S16 of ESI† for details.

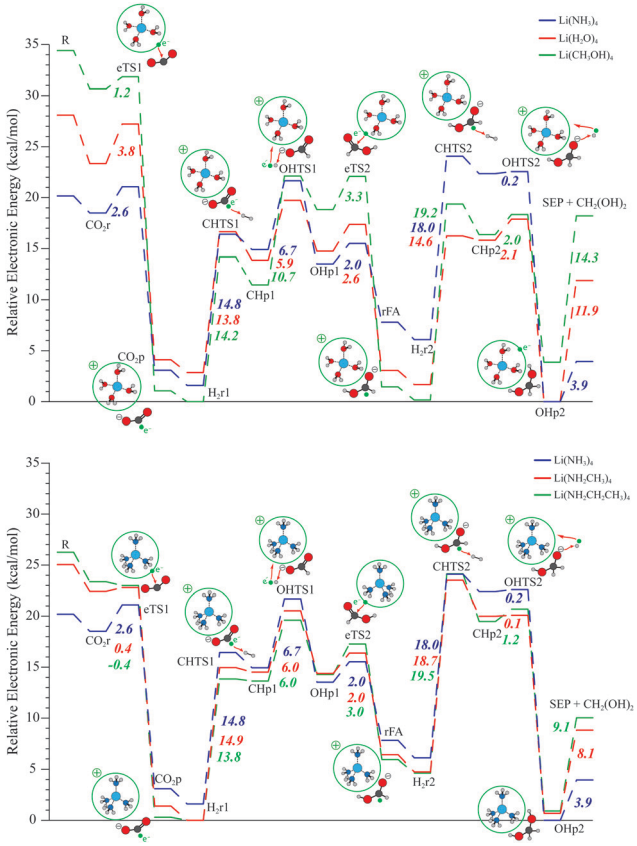

Fig. 2 Reaction pathways of $Li(X)_4$ + CO_2 + 2 H_2 → $Li(X)_4$ + $CH_2(OH)_2$, X = NH_3, NH_2CH_3, $NH_2CH_2CH_3$, H_2O, CH_3OH. Graphical representations of transition states and select intermediates are given as figure insets. A green dot is used to indicate the movement of the SEP e^- throughout the pathway. Activation barriers are given in kcal mol^{-1}. Relative electronic energies are zeroed to the lowest point of the pathway. See Table S16 of ESI† for details.

barrier (E_a) of the electron transfer is only 2.6 kcal mol^{-1}. After the transfer, an H_2 molecule binds to the complex (H_2r1). Subsequently, there is a transition state (CHTS1, E_a of 14.8 kcal mol^{-1}) involving the radical C of $CO_2^{\bullet -}$ attacking H_2 to form a C–H bond, breaking the H–H bond (CHp1). The next step is the transition state (OHTS1) involving the formation of an O-H bond and the return of an electron to the SEP (E_a of 6.7 kcal mol^{-1}) upon which formic acid (CHOOH) is formed. This may either be released, with a barrier of 6.2 kcal mol^{-1} (SEP + FA), or, with a barrier of 2 kcal mol^{-1} (eTS2), be reduced a second time to form $CHOOH^-$ (rFA). After the coordination of a second H_2 (H_2r2), a transition state involving the formation of a second C–H bond (CHTS2) with a barrier of 18 kcal mol^{-1} to form CH_2OOH^- (CHp2). This precedes the last transition state (OHTS2) of the O–H bond formation and the return of an electron to the $Li(NH_3)_4$ complex which has a barrier of 0.2 kcal mol^{-1}. This results in the formation of a methyldiol coordinated to the SEP which releases to form the separate products at a barrier of 3.9 kcal mol^{-1}.

This reaction in absence of the SEP proceeds slightly differently (see Fig. S1 of ESI†). Addition of each H_2 unit occurs in a single concerted transition state with an E_a = 13.8 kcal mol^{-1} for the first TS to give $CHOOH^-$ and E_a = 33.2 kcal mol^{-1} for the second to give $CH_2(OH)_2^-$. The first addition is lower in E_a than the combined two steps of the SEP mechanism (13.8 *vs.* 14.8 + 6.7); however, this is offset by the SEP's lower E_a barrier for the second H_2 (33.2 *vs.* 18 + 0.2). Additionally, the SEP serves an integral function in stabilizing the $CO_2^{\bullet -}$ radical. The electron affinity (EA) of CO_2 is −0.87 eV (−20.1 kcal mol^{-1}) which must first be overcome to proceed. When coordinated to $Li(NH_3)_4^+$, $CO_2^{\bullet -}$ is stabilized by 15.4 kcal mol^{-1} (CO_2p *vs.* CO_2r) over CO_2 coordinated to $Li(NH_3)_4$.

Shown in Fig. 2 is the effect of varying ligands on the reaction pathway. The ligands broken into two groups are: the hydroxy ligands (H_2O, CH_3OH) and the amine ligands (NH_3, NH_2CH_3, $NH_2CH_2CH_3$). These results indicate that the ligand choice significantly affects the pathway in only two areas: the initial electron transfer eTS and the dissociation of the products. Interchange of the ligands has no effect on the reaction mechanism and minimal effects (E_a within ± 3 kcal mol^{-1}) on the energetics of intermediate steps in the pathway (CO_2p through OHp2). Increasing the length of carbon chains in both the hydroxy and amine ligands results in an SEP electron which is more weakly bound and therefore more reductively reactive. The $Li(H_2O)_4$ complex possess the most tightly bound SEP electron with an ionization energy (IE calculated at CAM-B3LYP) of 3.67 eV to give the largest E_a for the electron transfer to CO_2 (eTS) at 3.8 kcal mol^{-1}. Addition of a methyl group (CH_3OH) lowers its IE to 3.36 eV and an E_a of eTS 1.2 kcal mol^{-1}. This trend is identical for the amine ligands NH_3: IE 3.02 eV & 2.6 kcal mol^{-1} E_a to NH_2CH_3: IE 2.76 eV & E_a

0.4 kcal mol^{-1} to $NH_2CH_2CH_3$: IE 2.59 eV. In the case of ethylamine, the SEP electron is bound so weakly that no barrier for the electron transfer exists. Finally, the hydroxy ligands more strongly coordinate the formic acid and methyldiol due to the stronger hydrogen bonds of O–H *vs.* N–H, requiring greater energy to dissociate the products.

Energetically, the H_2 pathway is electronically favorable; however, considering enthalpic and entropic effects the reaction is less so. At 298 K, the reaction is endothermic (ΔH) by 3.5 kcal mol^{-1} and endergonic (ΔG) by 12.5 kcal mol^{-1} (see Fig. S4–S7 of ESI† for details).

Transitioning to the ethene pathway, Fig. 3 depicts the reaction coordinate diagram for the conversion of CO_2 and ethene to a δ-lactone ring as catalyzed by the $Li(NH_3)_4$ and $Li(NH_2CH_3)_4$ SEPs. As in the H_2 system, the pathway begins with the reduction of CO_2 to a coordinated radical $CO_2^{\cdot-}$. Following which, an ethene coordinates to the complex (EtR) and is then attacked by the radical C of $CO_2^{\cdot-}$ (EtTS1, 9.0 and 9.1 kcal mol^{-1} E_a) to form a C–C bond, breaking the ethene π-bond and producing a terminal radical C (EtP). Following this, two things may occur: (1) The highest energy and least likely pathway involves a rearrangement (OHTS, 55.2 kcal mol^{-1} E_a) to produce a hydroxyl group and C–C double bond (OHEtP). (2) The process repeats (EtR2, EtTS2, and EtP2) to add a second ethene residue. Given that the barrier remains ∼9.0 kcal mol^{-1} for the addition of each ethene residue and that this addition is energetically downhill, either the C–C chain continues to grow as a polymerization reaction or, overcoming a barrier of 37.8/38.0 kcal mol^{-1} (LacTS), O attacks the terminal carbon to form the lactone ring and the radical electron is returned to the SEP. The subsequent step (LacP to P) involves the dissociation of lactone from the SEP - in the case of $Li(NH_2CH_3)_4$ this barrier is more than 3× that of $Li(NH_3)_4$ (5.8 *vs.* 19.1 kcal mol^{-1}).

As with the H_2 pathway, the ligand identity significantly affects only the first (eTS) and last step of the mechanism (P). The energetics and pathway of the intervening steps (SEPp through LacP) are virtually unaffected (E_a ±0.2 kcal mol^{-1}) by the ligand choice. The electronic energy activation barrier for the electron transfer to CO_2 (eTS) is smaller for methylamine due to its more weakly bound SEP electron, see above. In addition, the lactone dissociation from the methylamine complex is significantly harder due to it more strongly binding to the complex. The 38 kcal mol^{-1} barrier of LacTS will prove an initial hindrance at room temperature. This poses an avenue for future development and may be overcome through the tuning of reaction conditions, the use of ethene substituted by an electron donating functional group to promote a return of the electron to the SEP, or through the addition of further ethene residues before ring closure leading to a decrease in steric strain.

Overall, the ethene pathway offers far more promising results in terms of a viable catalytic cycle. The pathway at 298 K is exothermic by −22.3 kcal mol^{-1}. But due to the entropy penalty of converting three molecules (CO_2 + 2 C_2H_4) to one (δ-lactone) it is endergonic by 0.94 kcal mol^{-1} (for ΔG and ΔH plots see Fig. S8 and S9 of the ESI†). This naturally suggests several alternative reactants which may be used in place of ethene but should follow the same mechanism (Fig. 4). In reaction 1, the ethene pathway, three π-bonds (C═O and 2C═C) are broken to form three σ-bonds (C–O and 2C–C). In reaction 2, the use of a butadiene would decrease the entropic penalty (2 molecules → 1 molecule) but at the loss of an exothermic C–C σ-bond formation. Instead in reaction (3), the use of an octadiene would allow for the formation of the lactone ring and the three σ-bonds for an exothermic and exergonic reaction. In reaction (4), the o-xylylene and CO_2 reaction would lead to the formation of an aromatic ring-significantly increasing the free energy of the reaction at 298 K. In principle, the free energies must be calculated under the conditions that the stability of these systems is experimentally the largest, and future calculations will need input from experiment.

In summary, we provide insights into the application of SEPs as catalysts. We have used the reaction of CO_2 with H_2 and C_2H_4 as model systems for exploring this application.

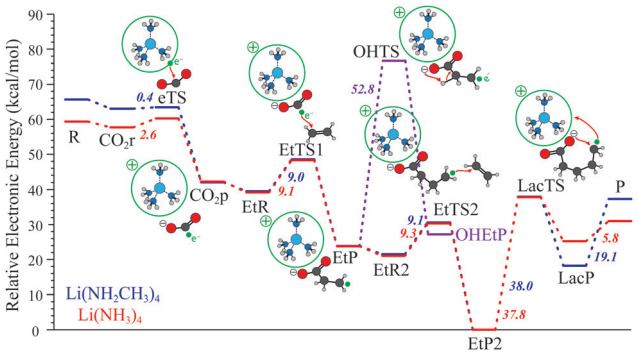

Fig. 3 Reaction pathways of $Li(NH_3/NH_2CH_3)_4$ + $2C_2H_4$ + $2CO_2$ → $Li(NH_3/NH_2CH_3)_4$ + $C_5H_8O_2$. Graphical representations of transition states and select intermediates are given as figure insets. A green dot is used to indicate the movement of the SEP e$^-$ throughout the pathway. Activation barriers are given in kcal mol^{-1}. Relative electronic energies are zeroed to the lowest point of the pathway. Shown in purple is a side reaction of the $Li(NH_2CH_3)_4$ system. See Table S17 of ESI† for details.

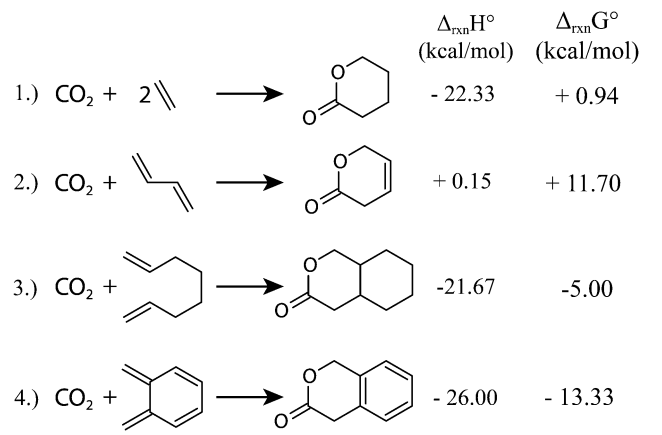

Fig. 4 Comparison of energetics for reactions analogous to the ethene pathway. Structures optimized at CAM-B3LYP. Basis sets: cc-pVTZ(C,O) aug-cc-pVTZ (H). See Tables S18 of ESI† for details.

Mechanisms for the conversion of CO_2 to formic acid/methyldiol and lactone as catalyzed by SEPs are proposed. The lithium-ligand SEP complex is shown to play an important role in stabilizing the reactant $CO_2^{\bullet -}$. Various ligands are tested, and ligand interchange is shown to have a significant effect on only two steps: the electron transfer (eTS) and the dissociation of products. The intervening steps are virtually independent of ligand identity. Increasing ligand size results in more diffuse solvated electrons and increased SEP reactivity. This degree of ligand interchange independence will allow future work to select ligands (hydroxy or amine) based on convenience. Additional insights from these results are used to propose additional reagents to produce spontaneous catalytic reactions. The CAM-B3LYP functional was benchmarked using the higher level CCSD(T) methodology and demonstrated excellent agreement in reaction energetics, validating the results herein. This work is meant to serve as a proof of concept, demonstrating the viability of SEPs in catalysis and providing insights for this application which may induce and inform future experimental work.

This material is based upon work supported by Auburn University (AU) and the National Science Foundation under Grant No. CHE-1940456. We acknowledge the support and resources provided by the Auburn University Hopper Cluster and Alabama Supercomputer Center.

Conflicts of interest

There are no conflicts to declare.

References

1 E. Zurek, P. P. Edwards and R. Hoffmann, *Angew. Chem., Int. Ed.*, 2009, **48**, 8198–8232.
2 H. E. Zimmerman, *Acc. Chem. Res.*, 2012, **45**, 164–170.
3 C. Van Der Linde, A. Akhgarnusch, C. K. Siu and M. K. Beyer, *J. Phys. Chem. A*, 2011, **115**, 10174–10180.
4 C. Van Der Linde, R. F. Höckendorf, O. P. Balaj and M. K. Beyer, *Chem. – Eur. J.*, 2013, **19**, 3741–3750.
5 T. W. Lam, C. Van Der Linde, A. Akhgarnusch, Q. Hao, M. K. Beyer and C. K. Siu, *ChemPlusChem*, 2013, **78**, 1040–1048.
6 E. Barwa, T. F. Pascher, M. Ončák, C. van der Linde and M. K. Beyer, *Angew. Chem., Int. Ed.*, 2020, **59**, 7467–7471.
7 S. Kar, A. Goeppert, V. Galvan, R. Chowdhury, J. Olah and G. K. S. Prakash, *J. Am. Chem. Soc.*, 2018, **140**, 16873–16876.
8 S. Kar, R. Sen, A. Goeppert and G. K. S. Prakash, *J. Am. Chem. Soc.*, 2018, **140**, 1580–1583.
9 G. A. Olah, G. K. S. Prakash and A. Goeppert, *J. Am. Chem. Soc.*, 2011, **133**, 12881–12898.
10 M. J. Frisch, G. W. Trucks, H. B. Schlegel, G. E. Scuseria, M. A. Robb, J. R. Cheeseman, G. Scalmani, V. Barone, G. A. Petersson, H. Nakatsuji, *et al.*, *Gaussian 16 Rev. C.01*, Wallingford, CT, 2016.
11 B. P. Prascher, D. E. Woon, K. A. Peterson, T. H. Dunning and A. K. Wilson, *Theor. Chem. Acc.*, 2011, **128**, 69–82.
12 D. E. Woon and T. H. Dunning, *J. Chem. Phys.*, 1995, **103**, 4572–4585.
13 R. A. Kendall, T. H. Dunning and R. J. Harrison, *J. Chem. Phys.*, 1992, **96**, 6796–6806.
14 T. Yanai, D. P. Tew and N. C. Handy, *Chem. Phys. Lett.*, 2004, **393**, 51–57.
15 S. N. Khan and E. Miliordos, *J. Phys. Chem. A*, 2020, **124**, 4400–4412.
16 B. A. Jackson and E. Miliordos, *J. Chem. Phys.*, 2021, **155**, 014303.
17 M. J. Frisch, M. Head-Gordon and J. A. Pople, *Chem. Phys. Lett.*, 1990, **166**, 275–280.
18 H.-J. Werner, P. J. Knowles, G. Knizia, F. R. Manby, M. Schütz, P. Celani, W. Györffy, D. Kats, T. Korona, R. Lindh, *et al.*, MOLPRO, version 2015.1, a package of *ab initio* programs, 2015.
19 J. D. Watts, J. Gauss and R. J. Bartlett, *J. Chem. Phys.*, 1993, **98**, 8718–8733.